

Figure 12 Measured antenna gain and simulated radiation efficiency for the proposed PIFA. (a) The lower band for GSM850/900 operation. (b) The upper band for GSM1800/1900/UMTS operation. [Color figure can be viewed in the online issue, which is available at www.interscience.wiley.com]

900 and GSM1800/1900/UMTS operations, respectively. Good radiation characteristics for frequencies over the operating bands have also been obtained. Detailed effects of the coplanar coupling feed on the antenna performances have also been analyzed.

REFERENCES

1. K.L. Wong, Planar antennas for wireless communications, Wiley, New York, 2003.
2. T. Oshiyama, H. Mizuno, and Y. Suzuki, Multi-band antenna, U.S. Pat Publ No. 2007/0249313 (2007).
3. J. Ollikainen, O. Kivekas, C. Icheln, and P. Vainikainen, Internal multiband handset antenna realized with an integrated matching circuit, Proc 12th Int Conf Antennas Propagat 2 (2003), 629–632.
4. M. Tzortzakakis and R.J. Langley, Quad-band internal mobile phone antenna, IEEE Trans Antennas Propagat 55 (2007), 2097–2103.
5. J. Villanen and P. Vainikainen, Optimum dual-resonant impedance matching of coupling element based mobile terminal antenna structures, Microwave Opt Technol Lett 49 (2007), 2472–2477.
6. J. Villanen, C. Icheln, and P. Vainikainen, A coupling element-based quad-band antenna element structure for mobile terminals, Microwave Opt Technol Lett 49 (2007), 1277–1282.
7. K.L. Wong, L.C. Chou, and C.M. Su, Dual-band flat-plate antenna with a shorted parasitic element for laptop applications, IEEE Trans Antennas Propagat 53 (2005), 539–544.
8. J. Ollikainen and A. Lehtola, Internal multi-band antenna with improved radiation efficiency, U.S. Pat No. 6,552,686 B2 (2003).
9. Y.X. Guo, M.Y.W. Chia, and Z.N. Chen, Miniature built-in multiband antennas for mobile handsets, IEEE Trans Antennas Propagat 52 (2004), 1936–1944.
10. K.L. Wong and Y.C. Lin, Thin internal planar antenna for GSM/DCS/PCS/UMTS operation in a PDA phone, Microwave Opt Technol Lett 47 (2005), 429–432.
11. K.L. Wong and C.H. Huang, Bandwidth-enhanced PIFA with a coupling feed for quad-band operation in the mobile phone, Microwave Opt Technol Lett 50 (2008), 683–687.
12. C.I. Lin and K.L. Wong, Printed monopole slot antenna for internal multiband mobile phone antenna, IEEE Trans Antennas Propagat 55 (2007), 3690–3697.
13. K.L. Wong, Y.C. Lin, and T.C. Tseng, Thin internal GSM/DCS patch antenna for a portable mobile terminal, IEEE Trans Antennas Propagat 54 (2006), 238–242.
14. K.L. Wong and C.H. Chang, Surface-mountable EMC monopole chip antenna for WLAN operation, IEEE Trans Antennas Propagat 54 (2006), 1100–1104.
15. K.L. Wong, Y.C. Lin, and B. Chen, Internal patch antenna with a thin air-layer substrate for GSM/DCS operation in a PDA phone, IEEE Trans Antennas Propagat 55 (2007), 1165–1172.
16. Y.L. Kuo and K.L. Wong, Printed double-T monopole antenna for 2.4/5.2 GHz dual-band WLAN operations, IEEE Trans Antennas Propagat 51 (2003), 2187–2192.
17. Available at: <http://www.ansoft.com/products/hf/hfss/>, Ansoft Corporation HFSS, 2008.

© 2008 Wiley Periodicals, Inc.

A HIGHER-ORDER OPTICAL TRANSFORMATION FOR NONMAGNETIC CLOAKING

Ilaria Gallina, Giuseppe Castaldi, and Vincenzo Galdi

Waves Group, Department of Engineering, University of Sannio, I-82100 Benevento, Italy; Corresponding author: vgaldi@unisannio.it

Received 4 April 2008

ABSTRACT: In coordinate-transformation-based approaches to electromagnetic concealment (“cloaking”) of objects, use of higher-order (quadratic) mappings has been proposed as an effective device to obtain satisfactory responses without the use of magnetic materials that are complicated to synthesize at optical frequencies. In this article, we explore a new higher-order algebraic transformation, which allows, in principle, for a broader range of applicability and further parametric optimization. Via full-wave numerical studies of near- and far-field observables, we assess its performance by comparison with various reference cases (nonreduced parameters, quadratic transformation, no cloak). © 2008 Wiley Periodicals, Inc. Microwave Opt Technol Lett 50: 3186–3190, 2008; Published online in Wiley InterScience (www.interscience.wiley.com). DOI 10.1002/mop.23905

Key words: electromagnetic cloaking; transformation optics; metamaterials; scattering

1. INTRODUCTION

During the past few years, transformation optics [1–3] has emerged as one among the most promising and active fields in optical and materials engineering, with the perspective of offering unprecedented control in the electromagnetic (EM) response of devices and components. Among the most exciting developments, besides the celebrated “invisibility cloaking” [4], it is worth mentioning “wormholes” [5], concentrators [6, 7], rotators [8], directive radiators [9], and optical devices [10–13].

The basic underlying idea is to design the desired field behavior in a fictitious space with a suitable (nonflat) topology, and then exploit the formal invariance of Maxwell's equations under coordinate transformations to interpret such a behavior in a conventional flat, Cartesian space filled by a suitable anisotropic, spatially inhomogeneous material which embeds the coordinate-transformation effects. For instance, in the cloaking application [14], where one is interested in rendering a volume of space "effectively invisible" to the impinging radiation, one starts from a fictitious space which contains a "hole." The great interest toward this cloaking strategy (see [15–22] for a sparse sampling of alternative approaches) is motivated by the rapid advances in the engineering of "metamaterials," with precise control of anisotropy and spatial inhomogeneity, which have recently allowed its experimental demonstration at microwave frequencies [4]. Moreover, exact full-wave studies [23, 24] have demonstrated that this approach is capable, in principle, of yielding perfect cloaking (i.e., zero external scattering and zero transmission into the concealment volume), though with strong sensitivity, with respect to perturbations [25] and simplifications/reductions [26] in the material parameters, and narrow bandwidth [27].

Recently, within the framework of scaling the above cloaking approach to optical frequencies [28], it was pointed out that the required magnetic properties of the metamaterial to be synthesized would pose significant technological challenges. Accordingly, an alternative approach was proposed [29], based on the use of a nonmagnetic material. Such an approach, capitalizing on the inherent arbitrariness in the choice of the coordinate-transformation, utilized a higher-order (quadratic, instead of linear [14]) mapping, with an additional degree of freedom which was exploited to enforce the impedance matching at the cloak interface with free space, thereby reducing the total scattering.

In this article, we elaborate on this idea, exploring a more general high-order optical transformation which allows, in principle, for a broader range of applicability and a further degree of freedom to optimize the response.

2. PROBLEM STATEMENT

Figure 1 illustrates the problem schematic in the associated Cartesian (x, y, z) and cylindrical (r, ϕ, z) coordinate systems. We consider a two-dimensional (2D) z -invariant scenario with a perfect electric-conducting (PEC) circular cylinder of radius R_1 surrounded by a cloaking shell of inner and outer radii R_1 and R_2 ,

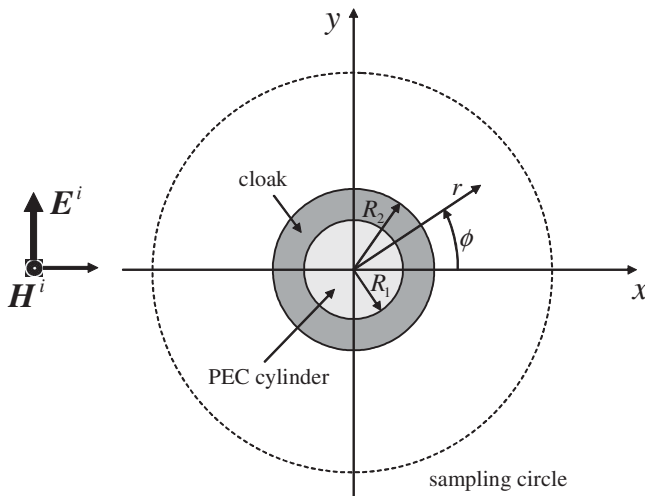


Figure 1 Problem schematic (details are discussed in the text)

respectively, in free space. We assume an incident plane wave along the positive x -direction, with time-harmonic ($\exp(i\omega t)$) dependence and transverse-magnetic (TM) polarization (magnetic field parallel to the cylinder). (Similar results can be obtained for the transverse-electric polarization, considering ϵ_z , μ_r , and μ_ϕ as the relevant constitutive parameters.)

A simple way to achieve cloaking is to define a cylindrical coordinate transformation $r = g(r')$, from (r', ϕ, z) to (r, ϕ, z) , which compresses the cylindrical region $r' \leq R_2$ into a concentric annulus $R_1 \leq r \leq R_2$ (i.e., satisfies the boundary conditions $g(0) = R_1$, $g(R_2) = R_2$). From the Jacobian matrix of the transformation, the constitutive parameters of the cloaking shell can readily be derived in terms of relative permittivity and permeability tensors [2, 14]. For the TM polarization, the relevant components (in cylindrical coordinates) are given by [29]

$$\epsilon_r(r) = \frac{r'}{r} \frac{dg(r')}{dr'}, \quad \epsilon_\phi(r) = \frac{1}{\epsilon_r(r)}, \quad \mu_z(r) = \frac{r'}{r} \left[\frac{dg(r')}{dr'} \right]^{-1}, \quad (1)$$

where $r' = g^{-1}(r)$ (with g^{-1} denoting the inverse mapping). In [29], a quadratic transformation was proposed (instead of the linear one in [14]),

$$g(r') = \left[1 - \frac{R_1}{R_2} + p(r' - R_2) \right] r' + R_1, \quad (2)$$

and a set of reduced nonmagnetic parameters was derived from (1) by multiplying ϵ_r and ϵ_ϕ by μ_z , yielding

$$\epsilon_r(r) = \left(\frac{r'}{r} \right)^2, \quad \epsilon_\phi(r) = \left[\frac{dg(r')}{dr'} \right]^{-2}, \quad \mu_z = 1. \quad (3)$$

(The underlying motivation is to preserve the ray trajectories inside the cloaking shell.) The extra degree of freedom p available in the quadratic transformation (2) was exploited to enforce the impedance-matching condition at the interface $r = R_2$,

$$\sqrt{\frac{\mu_z}{\epsilon_\phi(R_2)}} = \left. \frac{dg(r')}{dr'} \right|_{r'=g^{-1}(R_2)} = 1, \quad (4)$$

yielding $p = R_1/R_2^2$. Note that, to ensure the monotonicity of the transformation, the cloak "shape-factor" R_1/R_2 is restricted to values < 0.5 . Here, we propose an alternative higher-order algebraic transformation,

$$g(r') = \left[(R_2^\alpha - R_1^\alpha) \left(\frac{r'}{R_2} \right)^{\frac{1}{\gamma}} + R_1^\alpha \right]^{\frac{1}{\alpha}}, \quad (5)$$

and explore to what extent its more complex structure and the two parameters available (α and γ) can be exploited to broaden the range of applicability and optimize the response. Note that, like the quadratic transformation in (2), the proposed transformation in (5): (i) satisfies (for $\gamma > 0$) the required boundary conditions, and (ii) it yields perfect cloaking if the nonreduced constitutive parameters (1) are utilized [7]. However, unlike (2), the transformation in (5) is always monotonic (for $\alpha \neq 0$), regardless the cloak shape-factor R_1/R_2 . Enforcing the impedance-matching condition in (4) yields a relationship between the two parameters α and γ and the shape-factor,

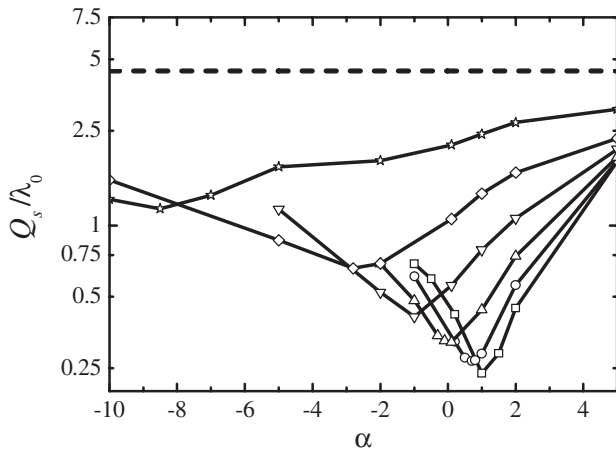


Figure 2 Total scattering cross-section per unit length (scaled to the free-space wavelength) for the proposed nonmagnetic cloak (with $R_1 = 0.98\lambda_0$), as a function of the parameter α , for various values of the shape-factor R_1/R_2 . Squares: $R_1/R_2 = 0.3$; circles: $R_1/R_2 = 0.4$; triangles: $R_1/R_2 = 0.5$; inverted triangles: $R_1/R_2 = 0.6$; diamonds: $R_1/R_2 = 0.7$; stars: $R_1/R_2 = 0.8$. As a reference, the dashed line indicates the value pertaining to the PEC cylinder alone (i.e., no cloak)

$$\gamma = \frac{1}{\alpha} \left[1 - \left(\frac{R_1}{R_2} \right)^\alpha \right], \quad (6)$$

which still leaves a free parameter for further optimization. In the following sections, we illustrate the results from a comprehensive parametric study, varying the cloak shape-factor and the transformation parameters.

3. REPRESENTATIVE RESULTS

To solve the EM scattering problem, we use a full-wave finite-element-method (FEM) commercial software [30] capable of handling anisotropic, inhomogeneous materials. In all simulations below, the PEC cylinder (and cloak inner-) radius R_1 is kept constant (as in [29]) to a value $R_1 = 0.98\lambda_0$ (with λ_0 denoting the free-space wavelength; the reference frequency value in all simulations is 2 GHz). The cloak shape-factor R_1/R_2 is varied from 0.3 (comparable to that in [29]) to 0.8.

As a compact meaningful observable of the scattering response, we consider the total scattering cross-section per unit length [20], which can be readily derived from the Bessel–Fourier expansion of the scattered magnetic field

$$H_z^{(s)}(r, \phi) = \sum_{m=-\infty}^{\infty} (-i)^m c_m H_m^{(2)}(k_0 r) \exp(im\phi), \quad (7)$$

as

$$Q_s = \frac{4}{k_0} \sum_{m=-\infty}^{\infty} |c_m|^2. \quad (8)$$

In (7) and (8), c_m denote the Bessel–Fourier expansion coefficients, $H_m^{(2)}$ is the m th-order Hankel function of the second kind [31], and $k_0 = 2\pi/\lambda_0$ denotes the free-space wavenumber. The expansion in (7) is derived via point-matching of the FEM full-wave solution on a near-zone circle of radius $6\lambda_0$ (see Fig. 1), with truncation dictated by spatial-bandwidth considerations [32].

Figure 2 shows the Q_s response (normalized with respect to the free-space wavelength) of the proposed nonmagnetic cloak as a function of the parameter α (with γ given by the impedance-matching condition (6)), for different values of the shape-factor R_1/R_2 , together with the reference level pertaining to the PEC cylinder alone (i.e., without any cloak). It is observed that, although the impedance at the interface between the cloak and free-space is always matched (in view of (6)), the response can vary significantly with the parameter α . Interestingly, the curves exhibit similar trends, with well-defined minima for specific values of α . As the shape-factor increases, the minima tend to become broader and to move toward negative values of α . Moreover, the optimal values of Q_s tend to increase. This can be intuitively expected in view of the reduced thickness of the cloak, which renders less effective the waveguiding of energy around the PEC cylinder. Nevertheless, for shape-factors up to $R_1/R_2 = 0.7$, one still observes a total scattering cross-section about an order of magnitude smaller than in the absence of the cloak, and, even in the particularly challenging $R_1/R_2 = 0.8$ case, a reduction of about a factor 4 is achieved.

In Table 1, the minimum values $Q_s^{(\min)}/\lambda_0$ are reported and compared, whenever possible, with the corresponding reference values $Q_s^{(\text{ref})}/\lambda_0$ obtained using the quadratic transformation (2) (cf. [29]). (For the quadratic transformation, the value pertaining to $R_1 = R_2 = 0.5$ was actually computed at $R_1 = R_2 = 0.499$ in order to ensure the monotonicity.) Once again, it is emphasized that the proposed cloak is not restricted to shape-factors $R_1/R_2 < 0.5$. Moreover, within the range of applicability of the quadratic transformation, it always yields moderately smaller values of Q_s , with reduction factors ranging from 1.6 to 1.2.

To complete the parametric study, we also looked at the near-field distribution. Figure 3 shows the radial component of the FEM-computed Poynting vector on a circle of radius $6\lambda_0$ (see Fig. 1), for the proposed cloak with nonreduced (cf. (1)) and nonmagnetic (cf. (3)), with α chosen so as to minimize the total scattering cross-section, and γ given by (6) parameters, as well as for the PEC cylinder alone, as a function of the observation angle ϕ , for various values of the shape-factor R_1/R_2 . (In our simulations, we chose $\alpha = 3$ and $\gamma = 2$, but any arbitrary combination of parameters should work in the nonreduced case.) All scattering patterns are normalized with respect to the response maximum of the PEC cylinder alone. Note that the nonzero, albeit very small, scattering response of the ideal cloak with nonreduced parameters is attributable to the inherently limited precision of the full-wave FEM solver.

Similar observations as for the far-field case can be made. When compared with the PEC cylinder alone, a reduction in the scattering response is always achieved for all the shape-factors and observation directions, ranging from about an order of magnitude

TABLE 1 Minimum (Over α) Total Scattering Cross-Section per Unit Length $Q_s^{(\min)}/\lambda_0$ (Scaled to the Free-Space Wavelength) for the Proposed Nonmagnetic Cloaking, Compared With the Reference Value $Q_s^{(\text{ref})}$ Obtained Using the Quadratic Transformation [29], for Various Values of the Shape-Factor

R_1/R_2	$Q_s^{(\min)}/\lambda_0$	$Q_s^{(\text{ref})}/\lambda_0$
0.3	0.238	0.387
0.4	0.268	0.382
0.5	0.322	0.379
0.6	0.412	–
0.7	0.660	–
0.8	1.173	–

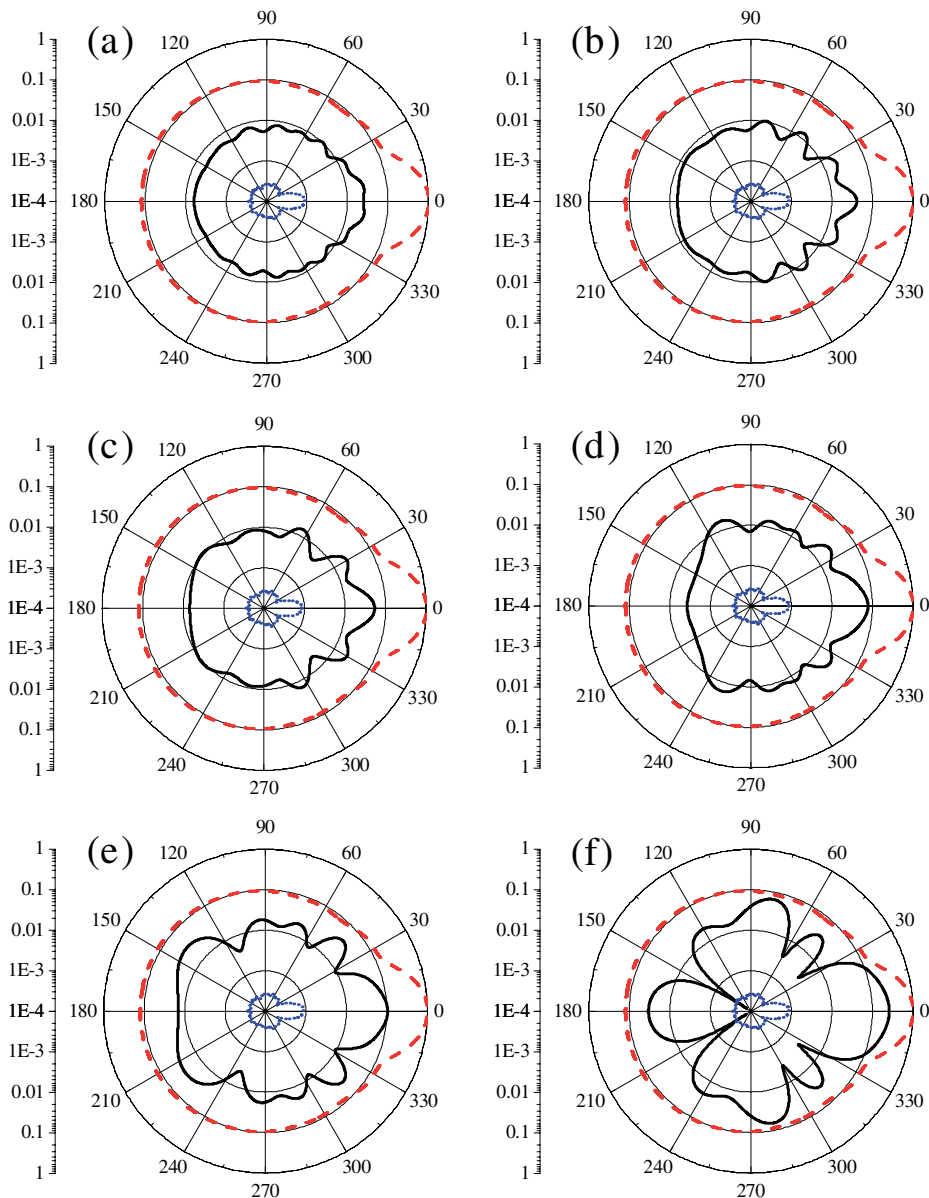


Figure 3 Radial component of the near-zone ($r = 6\lambda_0$) Poynting vector for the proposed nonmagnetic cloaking (with α chosen so as to minimize the total scattering cross-section, and γ given by (6)) for various values of the shape-factor R_1/R_2 (black continuous curves). (a) $R_1/R_2 = 0.3$; (b) $R_1/R_2 = 0.4$; (c) $R_1/R_2 = 0.5$; (d) $R_1/R_2 = 0.6$; (e) $R_1/R_2 = 0.7$; (f) $R_1/R_2 = 0.8$. Also shown, as references, are the responses pertaining to the PEC cylinder alone (red dashed curves), and the nonreduced-parameter cloaking with $\alpha = 3$ and $\gamma = 2$ (blue dotted curves). All curves are normalized with respect to the response maximum of the PEC cylinder alone. [Color figure can be viewed in the online issue, which is available at www.interscience.wiley.com]

(for $R_1/R_2 \leq 0.7$) to nearly a factor of 4 (for $R_1/R_2 = 0.8$, in most directions).

From the above results, the proposed higher-order nonmagnetic cloak turns out to be satisfactorily applicable to a fairly broad range of shape-factors.

4. CONCLUSIONS

In this article, we have dealt with the study of a higher-order optical transformation for 2D nonmagnetic cloaking. Via full-wave studies of the near- and far-field responses, we have explored its range of applicability, addressed its parametric optimization, and assessed its performance, by comparison with various reference cases (nonreduced parameters, quadratic transformation, PEC cylinder alone). Overall, the proposed cloak turns out to provide

sensible reductions in the scattering response over a rather wide parametric range.

We stress that no attempt was made at this stage to deal with actual fabrication-oriented issues. In this connection, some technological challenges could be expected for higher values of the shape-factor (i.e., thinner cloaking shells), in view of the possibly strong permittivity gradients that could be required.

Current and future investigations are aimed at the exploration of different higher-order transformations, also for other applications (e.g., hyperlenses).

ACKNOWLEDGMENT

The assistance of Dr. Bruno Bisceglia (University of Salerno, Italy) in the full-wave simulations is gratefully acknowledged.

REFERENCES

1. D. Schurig, J.B. Pendry, and D.R. Smith, Calculation of material properties and ray tracing in transformation media, *Opt Express* 14 (2006), 9794–9804.
2. U. Leonhardt and T.G. Philbin, General relativity in electrical engineering, *New J Phys* 8 (2006), 247.
3. U. Leonhardt, Optical conformal mapping, *Science* 312 (2006), 1777–1780.
4. D. Schurig, J.J. Mock, B.J. Justice, S.A. Cummer, J.B. Pendry, A.F. Starr, and D.R. Smith, Metamaterial electromagnetic cloak at microwave frequencies, *Science* 314 (2006), 977–980.
5. A. Greenleaf, Y. Kurylev, M. Lassas, and G. Uhlmann, Electromagnetic wormholes and virtual magnetic monopoles from metamaterials, *Phys Rev Lett* 99 (2007), 183901.
6. M. Rahm, D. Schurig, D.A. Roberts, S.A. Cummer, D. R. Smith, and J.B. Pendry, Design of electromagnetic cloaks and concentrators using form-invariant coordinate transformations of Maxwell's equations, *Photon Nanostruct – Fundam Appl* 6 (2008), 87–95.
7. A.D. Yaghjian and S. Maci, Alternative derivation of electromagnetic cloaks and concentrators, in press; arXiv:0710.2933v4 [physics.class-ph].
8. H.Y. Chen and C.T. Chan, Transformation media that rotate electromagnetic fields, *Appl Phys Lett* 90 (2007), 241105.
9. Y. Luo, J. Zhang, L. Ran, H. Chen, and J.A. Kong, Controlling the emission of electromagnetic sources by coordinate transformation, in press; arXiv:0712.3776v1 [physics.optics].
10. D. Schurig, J.B. Pendry, and D.R. Smith, Transformation-designed optical elements, *Opt Express* 15 (2007), 14772–14782.
11. A.V. Kildishev and E.E. Narimanov, Impedance-matched hyperlens, in press; arXiv:0708.3798v1 [physics.optics].
12. M. Tsang and D. Psaltis, Magnifying perfect lens and superlens design by coordinate transformation, *Phys Rev B* 77 (2008), 035122.
13. A.V. Kildishev and V.M. Shalaev, Engineering space for light via transformation optics, *Opt Lett* 33 (2008), 43–45.
14. J.B. Pendry, D. Schurig, and D.R. Smith, Controlling electromagnetic fields, *Science* 312 (2006), 1780–1782.
15. P.-S. Kildal, A. Kishk, and A. Tengs, Reduction of forward scattering from cylindrical objects using hard surfaces, *IEEE Trans Antennas Propagat* 44 (1996), 1509–1520.
16. D.A.B. Miller, On perfect cloaking, *Opt Express* 14 (2006), 12457–12466.
17. A. Alù and N. Engheta, Plasmonic materials in transparency and cloaking problems: Mechanism, robustness, and physical insights, *Opt Express* 15 (2007), 3318–3332.
18. Y. Huang, Y. Feng, and T. Jiang, Electromagnetic cloaking by layered structure of homogeneous isotropic materials, *Opt Express* 15 (2007), 11133–11141.
19. A. Hakansson, Cloaking of objects from electromagnetic fields by inverse design of scattering optical elements, *Opt Express* 15 (2007), 4328–4334.
20. M.G. Silveirinha, A. Alù, and N. Engheta, Parallel-plate metamaterials for cloaking structures, *Phys Rev E* 75 (2007), 036603.
21. N.A.P. Nicorovici, G.W. Milton, R.C. McPhedran, and L.C. Botten, Quasistatic cloaking of two-dimensional polarizable discrete systems by anomalous resonance, *Opt Express* 15 (2007), 6314–6323.
22. P. Alitalo, O. Luukkainen, L. Jylha, J. Venermo, and S.A. Tretyakov, Transmission-line networks cloaking objects from electromagnetic fields, *IEEE Trans Antennas Propagat* 56 (2008), 416–424.
23. H.S. Chen, B.I. Wu, B. Zhang, and J.A. Kong, Electromagnetic wave interactions with a metamaterial cloak, *Phys Rev Lett* 99 (2007), 063903.
24. B. Zhang, H.S. Chen, B.I. Wu, Y. Luo, L.X. Ran, and J.A. Kong, Response of a cylindrical invisibility cloak to electromagnetic waves, *Phys Rev B* 76 (2007), 121101.
25. Z. Ruan, M. Yan, C.W. Neff, and M. Qiu, Ideal cylindrical cloak: Perfect but sensitive to tiny perturbations, *Phys Rev Lett* 99 (2007), 113903.
26. M. Yan, Z.C. Ruan, and M. Qiu, Cylindrical invisibility cloak with simplified material parameters is inherently visible, *Phys Rev Lett* 99 (2007), 233901.
27. H.Y. Chen, Z.X. Liang, P.J. Yao, X.Y. Jiang, H.R. Ma, and C.T. Chan, Extending the bandwidth of electromagnetic cloaks, *Phys Rev B* 76 (2007), 241104.
28. W.S. Cai, U.K. Chettiar, A.V. Kildishev, and V.M. Shalaev, Optical cloaking with metamaterials, *Nat Photon* 1 (2007), 224–227.
29. W. Cai, U.K. Chettiar, A.V. Kildishev, V.M. Shalaev, and G.W. Milton, Nonmagnetic cloak with minimized scattering, *Appl Phys Lett* 91 (2007), 111105.
30. COMSOL Multiphysics—User's Guide, COMSOL AB, 2005.
31. M. Abramowitz and I.A. Stegun, *Handbook of mathematical functions*, Dover, New York, NY, 1964.
32. O.M. Bucci and G. Franceschetti, On the degrees of freedom of scattered fields, *IEEE Trans Antennas Propagat* 37 (1989), 918–926.

© 2008 Wiley Periodicals, Inc.

EXPERIMENTAL VALIDATION OF PERCOLATION-BASED MODELS FOR PROPAGATION PREDICTION

R. Azaro, A. Martini, and A. Massa

ELEDIA Research Group Department of Information and Communication Technology University of Trento, Via Sommarive 14, I-38050 Trento, Italy; Corresponding author: andrea.massa@ing.unitn.it

Received 12 April 2008

ABSTRACT: In this letter, an experimental validation of percolation-based approaches for the prediction of wave propagation in random media is presented. Measurements are collected in a real controlled environment, where the obstacles are stochastically placed in a two-dimensional grid according to a known nonuniform density distribution. The obtained results show that, in spite of their simplicity, percolation-based approaches can be applied in real propagation problems. © 2008 Wiley Periodicals, Inc. *Microwave Opt Technol Lett* 50: 3190–3192, 2008; Published online in Wiley InterScience (www.interscience.wiley.com). DOI 10.1002/mop.23937

Key words: percolation theory propagation; stratified random media; electromagnetic propagation; experimental validation

1. INTRODUCTION

The prediction of e.m. propagation in disordered distributions of obstacles is a challenging research topic [1]. A possible approach to such a topic consists of modeling the propagation environment by means of a percolation lattice [2] and describing the propagation through a stochastic process. This allows one to obtain analytical closed-form solutions that describe the average properties of the e.m. propagation [3, 4]. With reference to the far-external source scenario and under the assumption that the obstacles are nonuniformly distributed, this letter is aimed at presenting the results of an experimental validation performed in a real controlled environment to validate the percolation-based solutions [5, 6].

2. SETUP

The experiments have been carried out in an anechoic chamber, 6 m long, 3 m wide, and 4 m high, available at the ELEDIA laboratory. Sketch and wide-angle shot of the experimental setup are given in Figures 1 and 2, respectively. A 2 m-sided square area has been partitioned in $K = 10$ rows, each one containing $I = 10$ cells. Obstacle were polystyrene cylinders with square section (0.2 m \times 0.2 m), 2 m high, lined with a metallic film. The transmitting device, aimed at modeling the e.m. source, was an Oritel ANC 100/15 dB pyramidal horn antenna whose dimensions have been